





# Landslide initiation and runout susceptibility modeling in the context of hill cutting and rapid urbanization: a combined approach of weights of evidence and spatial multi-criteria

**RAHMAN Md. Shahinoor**<sup>1,2</sup>  <http://orcid.org/0000-0001-5540-3307>; e-mail: mrahma25@masonlive.gmu.edu

**AHMED Bayes**<sup>3,4</sup>  <http://orcid.org/0000-0001-5092-5528>; e-mail: bayesahmed@gmail.com

**DI Liping**<sup>1\*</sup>  <http://orcid.org/0000-0002-3953-9965>;  e-mail: ldi@gmu.edu

\* Corresponding author

<sup>1</sup> Center for Spatial Information Science and Systems, George Mason University, Fairfax, VA 22030, USA

<sup>2</sup> BUET-Japan Institute of Disaster Prevention and Urban Safety, Bangladesh University of Engineering and Technology (BUET), Dhaka 1000, Bangladesh

<sup>3</sup> Institute for Risk and Disaster Reduction, Department of Earth Sciences, University College London (UCL), Gower Street, London WC1E 6BT, UK

<sup>4</sup> Department of Disaster Science and Management, Faculty of Earth and Environmental Sciences, University of Dhaka, Dhaka 1000, Bangladesh

**Citation:** Rahman MS, Ahmed B, Di L (2017) Landslide initiation and runout susceptibility modeling in the context of hill cutting and rapid urbanization: a combined approach of weights of evidence and spatial multi-criteria. *Journal of Mountain Science* 14(10). <https://doi.org/10.1007/s11629-016-4220-z>

© Science Press and Institute of Mountain Hazards and Environment, CAS and Springer-Verlag GmbH Germany 2017

**Abstract:** Rainfall induced landslides are a common threat to the communities living on dangerous hill-slopes in Chittagong Metropolitan Area, Bangladesh. Extreme population pressure, indiscriminate hill cutting, increased precipitation events due to global warming and associated unplanned urbanization in the hills are exaggerating landslide events. The aim of this article is to prepare a scientifically accurate landslide susceptibility map by combining landslide initiation and runout maps. Land cover, slope, soil permeability, surface geology, precipitation, aspect, and distance to hill cut, road cut, drainage and stream network factor maps were selected by conditional independence test. The locations of 56 landslides were collected by field surveying. A weight of evidence (WoE) method was applied to calculate the positive (presence of landslides) and negative (absence of

landslides) factor weights. A combination of analytical hierarchical process (AHP) and fuzzy membership standardization (weights from 0 to 1) was applied for performing a spatial multi-criteria evaluation. Expert opinion guided the decision rule for AHP. The Flow-R tool that allows modeling landslide runout from the initiation sources was applied. The flow direction was calculated using the modified Holmgren's algorithm. The AHP landslide initiation and runout susceptibility maps were used to prepare a combined landslide susceptibility map. The relative operating characteristic curve was used for model validation purpose. The accuracy of WoE, AHP, and combined susceptibility map was calculated 96%, 97%, and 98%, respectively.

**Keywords:** Landslide susceptibility; Landslide runout; GIS; Remote sensing; Weights of evidence (WoE); Analytical hierarchical process (AHP); Relative operating characteristic (ROC); Bangladesh

**Received:** 21 September 2016

**Revised:** 26 October 2016

**Accepted:** 14 July 2017

## Introduction

Landslides hit Chittagong Metropolitan Area (CMA), Bangladesh almost every year, particularly during the monsoon period (June–September). Most recently on 13 June 2017, a series of landslides killed at least 160 people in various hilly districts in Chittagong division. On 19 July 2015, three people were killed because of a landslide in Lalkhan Bazaar area (Figure 1), Chittagong. Flash flooding triggered by heavy rainfall caused this landslide. The main causes of landslides in CMA are associated with hill cutting and development of housing blocks on risky hill-slopes violating the existing urban master plan (Ahmed 2015a). Notably, on 11 June 2007, eight days of continuous rainfall (610 mm) triggered landslides in different parts of CMA and caused 128 casualties and at least 100 injuries. Ninety people were killed on 26 June 2012 due to rainfall-triggered (8 days of 889 mm) landslides in CMA. Large to small-scale landslide disasters are gradually becoming evident in CMA. It is necessary to address landslide disaster risk reduction (DRR) strategies in CMA. Preparing a scientifically valid landslide susceptibility map could be considered as the first step.

Even being located in a high-risk zone for earthquakes (Steckler et al. 2016), landslides are primarily caused by torrential rainfall in CMA. Also, being the second largest city in Bangladesh, a compact mono-centric urban area is attracting huge numbers of people in search of livelihoods. CMA is surrounded by the Bay of Bengal to the west, and the remaining land area is not plain. Land prices are extremely high and out of reach of middle to lower-income people because of overwhelming population pressure with severe land scarcity and people looking for economic opportunities. Land grabbers are systematically approaching to destroy the hills in CMA by promoting business in selling plots and flats. They are also making full use of the marginalized people who are migrating to the city in search of better livelihood opportunities or who have lost their lands in river erosion or who are victims of other disasters in different parts of the country (e.g. drought, sea-level rise, riverbank erosion, river flooding and flash floods, or cyclones). The disaster-hit people are forced to live in hazardous locations in the city. By-law, only the government owns the hills in Bangladesh, and it is not possible to build houses on the hill slopes. The landlords



**Figure 1** Landslide devastation on 19 July 2015 in Chittagong Metropolitan Area. Source: Fieldwork, July 2015.

strategically guide the migrating urban-poor to those hills by providing illegal housing and other utility facilities for living temporarily. Later the local authorities fail to evacuate them on humanitarian ground. By this way, informal settlements start growing on the hills, and later a group of powerful people cut the hills gradually. After years, when the hills disappear, there is no other way than permitting multi-storied buildings in the newly created flatlands converting from the hills. This is the overall hill cutting scenario in CMA over the past few decades (Ahmed and Dewan 2017; BUET-JIDPUS 2015). Although landslides hazards are mostly natural events but vulnerability at community scale (Alexander 2000) is primarily triggering landslide disasters in Bangladesh. At this background, the aim of this research article is to prepare landslide susceptibility maps (LSMs). It would help to demarcate the susceptible zones to landslides in CMA. The context is set to hill cutting in highly urbanized areas in a developing country. This context is unique and needs attention in the perspective of landslide susceptibility mapping (LSM) and landslide DRR.

### 1 Study Area

CMA is located in the Chittagong district (Figure 2a), sharing a boundary with the Hindu Kush Himalayan region. CMA is situated between approximate 22°06' and 22°34' N, and 91°40' and 92°2' E. Karnafuli River runs from the east towards south-west, and the Halda River runs from north to south direction and joins the Karnafuli River before it flows into the Bay of Bengal (Figure 2b). CMA accommodates about 5 million people in approximate 720 km<sup>2</sup> area (BBS 2012). The development control authority of CMA is known as Chittagong Development Authority (CDA). The annual average temperature of Chittagong district is 32.5°C (maximum) and 13.5°C (minimum).

Chittagong is different regarding topography, from the rest of Bangladesh, being a part of the hilly regions that branch off from the Himalayas. This eastern offshoot of the Himalayas, turning south and southeast and enters Chittagong district. The range loses height as it approaches CMA and breaks up into small hillocks scattered all over the town. This range appears again on the southern

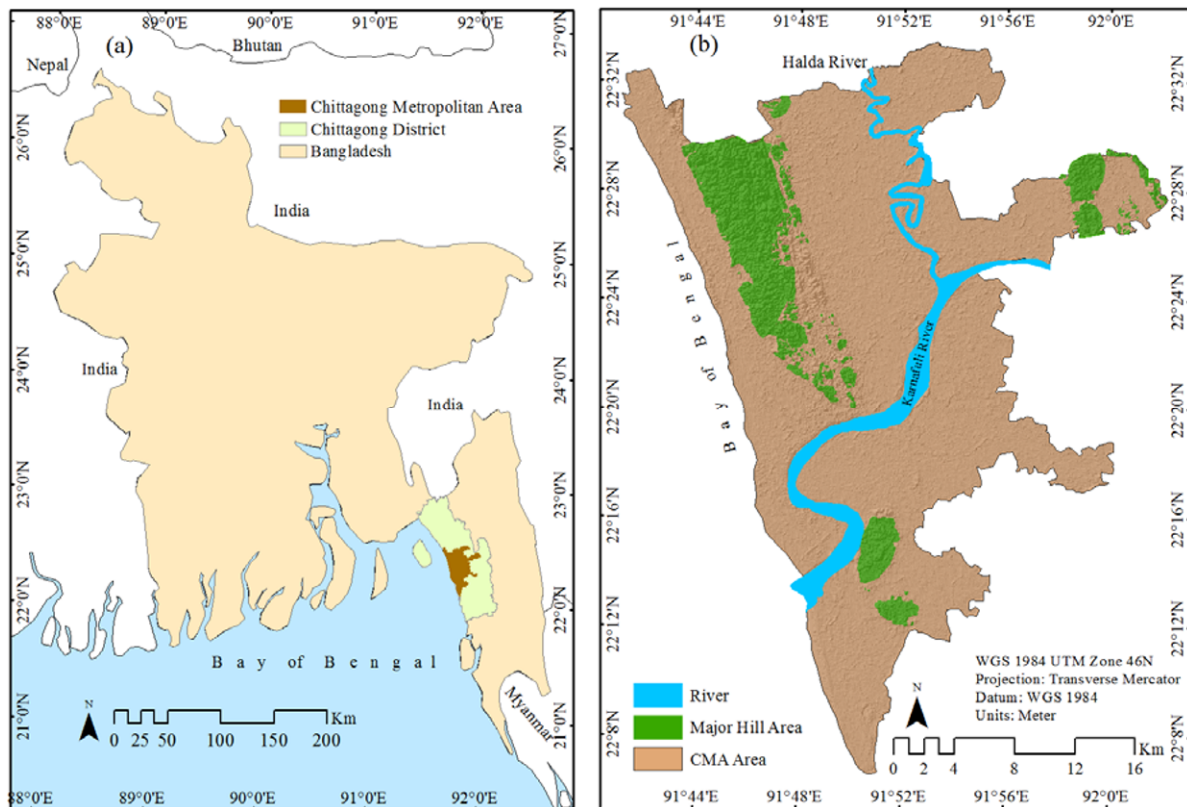


Figure 2 (a) Location of Chittagong Metropolitan Area (CMA) in Chittagong district, and (b) location of CMA.

bank of the Karnafuli River and extends from one end of the district to the other. The highest peak in the district has an altitude of 351 meters above the mean sea level. The beautiful hills and hillocks in the city of Chittagong are gradually leveled up and reduced in height for the construction of houses (Osmany 2014). The soils of the hills in CMA are primarily composed of sand (about 20%-65%), silt (15%-30%) and clay (36%-82%) (Ahmed and Rubel 2013; BUET-JIDPUS 2015).

The geosynclinal basin in the southeast of Bangladesh (that covers the study area) is characterized by the huge thickness (maximum of about 20 km near the basin center) of clastic sedimentary rocks, mostly sandstone and shale of Tertiary age. The huge thickness of sediments in the basin is a result of tectonic mobility or instability of the areas causing rapid subsidence and sedimentation in a relatively short span of geologic time. The anticlines form the hills, and the synclines form valleys as seen in the topography of the eastern regions of Bangladesh. The intensity of the folding is greater towards the east, causing a higher topographic elevation in the eastern Chittagong hill tracts (Imam 2015).

The annual average rainfall is about 2900 mm (BBS 2012). The pre-monsoon season is from April-May, and the monsoon season is from June to October which is warm, cloudy and wet. After analyzing the rainfall pattern (1950-2013) in Chittagong district, the following statistics (average) were calculated (Ahmed and Dewan 2017):

- Monthly maximum 1-day precipitation = 236 mm.
- Monthly maximum consecutive 5-day precipitation = 490 mm.
- Number of heavy precipitation days (precipitation  $\geq 10$  mm) = 61 days.
- Number of very heavy precipitation days (precipitation  $\geq 20$  mm) = 41 days.
- Number of days above 50 mm = 18 days.
- Consecutive wet days = 15 days.

It is likely to rain heavily ( $\geq 20$  mm) for at least 41 days and to rain for 15 consecutive days in CMA during the monsoon. The gradual upward trends of population pressure, indiscriminate hill cutting and deforestation, rapid urbanization in the physically vulnerable hills, and the likeliness of increasing the heavy precipitation events are posing serious threats of landslides in CMA.

## 2 Materials and Methods

### 2.1 Theoretical framework

To begin with, it is important to determine the potential locations of landslides (i.e. landslide initiation zones), and the probable post-failure movement (i.e. runout) of the slide (Zahra 2010; Petrascheck and Kienholz 2003). A landslide is defined as a movement of a mass of soil or earth down a slope. Susceptibility is defined as a quantitative or qualitative assessment of the classification, area or volume, and spatial distribution of landslides that exist or potentially can occur in an area (Fell et al. 2008). Runout is the maximum travel distance of a landslide (Couture 2011). Infrastructure and facilities mostly tend to be located in the toe of a slope that is vulnerable to displaced mass (Willenberg et al. 2009). It is essential to know where, how far and how fast a landslide could travel once mobilized (Dai et al. 2002).

Determining the spatial and temporal probability of a landslide is growing interest among researchers (Rickenmann 2005; Kappes et al. 2011; Soeters and van Westen 1996). Beguería et al. (2009) mentioned that a landslide system is theoretically divided into three components – initiation zone, travel zone, and deposition zone. Spatial distribution of these zones is important in LSM. This study aims to identify the probable landslide initiation zone of CMA and the associated spatial distribution of runout from the mass movement of the initiation zone. With the advancement of geographic information system (GIS) and remote sensing (RS) techniques and availability of datasets – LSM has become popular (Ahmed 2015b). Both data-driven statistical (i.e. weights of evidence, logistic regression, multiple logistic regression) and weight based techniques such as artificial hierarchy process (AHP), weighted linear combination (WLC), and ordered weighted average (OWA) are also being implemented for LSM (Fan et al. 2017; Du et al. 2017; Regmi et al. 2016; Meten et al. 2015; Bai et al. 2013).

Zahra (2010) summarized various runout modeling techniques grouped into three mainstream approaches as identified by Chen and Lee (2004), namely– empirical approach, physical

scale modeling, and dynamic modeling. There exists several models for debris flow propagation assessment, empirical mass change (Dai et al. 2002), empirical angle of reach method (Prochaska et al. 2008), analytical lumped mass model (Chen and Lee 2004), numerical distinct element method (Wong and Ho 1996), and numerical continuum models (Dai et al. 2002; Chen and Lee 2004). A continuum numerical approach includes conservation equations for mass, momentum, energy, and dynamic motion of displaced mass along with the rheological models (Dai et al. 2002) where the estimation of an appropriate rheological model is a difficult part (Zahra 2010). On the contrary, physical based models are used for both large, deep, complex and shallow landslides where model parameters are derived from field measurement, and high data volume is required (Brunsdon 1999). However, among the sophisticated techniques that are available for debris flow propagation assessment (Pirulli and Mangeney 2008; Hungr 1995; Iovine et al. 2005), few are suitable for regional-scale level analysis (Van Westen et al. 2006; Berti and Simoni 2007). The main limitations of these sophisticated models are high volume and detail data requirement. Horton et al. (2013) mentioned that process modeling is not suitable for regional-scale assessment due to the complex nature of the phenomenon, the variability of local controlling factors, and uncertainty of modeling parameters. A simplified approach that is not highly parameter dependent is suitable for regional-scale runout modeling. In this study, a distributed empirical model is selected for the runout susceptibility analysis of CMA using a digital elevation model (DEM). A similar method was successfully applied in different case studies to provide a substantial basis for landslide susceptibility assessment at a regional scale (Horton et al. 2013). This study is also going to apply a combined approach incorporating both knowledge and data driven techniques for landslide susceptibility modeling.

## 2.2 Landslide inventory mapping

Information on past landslides is required for model running and validation purposes. Van Westen et al. (2008) mentioned the importance of a comprehensive landslide inventory to quantify

both landslide hazard and risk. Past landslide is useful for LSM which can be seen as the opportunity (Rahman and Kausel 2012) to learn the lesson for the future. Previously, only few landslide locations (point data) of CMA were documented (Ahmed and Rubel 2013). There was no complete landslide area (polygon) based inventory. An initiative of BUET-Japan Institute of Disaster Prevention and Urban Safety (BUET-JIDPUS) prepared and published a detailed landslide inventory of 56 landslides of the study area through field survey in July–August 2014 (Rahman et al. 2016; Ahmed et al. 2014). The published inventory is considered for this study which covers the historical landslide locations, landslide width, length, mechanism, damage, and landuse pattern (Rahman et al. 2016; Ahmed et al. 2014). A total of 56 landslides were identified using a Global Positioning System (GPS) device (Figure 3a). The landslide locations were divided into two sets based on random selection— 50% of those were categorized as training landslides and the second half was considered as a test dataset. Training dataset is used as an input factor for data-driven WoE analysis, and test dataset is used for the validation of the LSM outcomes.

## 2.3 Hill cut mapping

The context of this study is hill cutting, urbanization, and associated landslides. Until now, works published on landslides in Chittagong city (Chisty 2014; Mia et al. 2016; Rahman et al. 2016; Ahmed and Rubel 2013) mentioned extensively on uncontrolled hill cutting activities and rapid urbanization as the primary causes for recent landslides. Those works did not consider hill cutting map as a factor. A hill cutting map for CMA was prepared to incorporate in LSM for better understanding the overall landslide situation. Satellite images were analyzed to identify hill cutting from 1990-2010. Hill cutting activities were historically accelerated due to urbanization and deforestation (Ahmed 2015a). It is assumed that land cover type converted from hill forest (or hills covered by dense vegetation) to urban areas were primarily due to hill cutting.

Landsat 4–5 thematic mapper images dated – 31 October 1990 and 23 November 2010 (row 136, and path 44 and 45) were downloaded from the

global visualization viewer of the United States Geological Survey (USGS). The images were then projected using WGS-1984 datum and UTM Zone 46 North coordinate system. Images were collected from the late autumn because this season is generally cloud free and trees are not in the leaf-off condition in the context of local climate. A supervised image classification method was applied to classify images into six broad land cover classes namely – built-up areas (urban and rural), hill forest, shrub land, crop land, bare soil, and water body (Ahmed et al. 2013; Ahmed and Ahmed 2012).

To minimize the misclassification of asphalt surfaces, water bodies were extracted separately through band addition and threshold estimation techniques of near infrared and mid-infrared band of Landsat TM. A water layer mask was applied to improve the land cover maps (Rahman and Di 2017). A post classification change detection method was applied to identify the changes of land cover classes. After analyzing the context, only the change from hill forest to an urban area (1990-2010) was considered for hill cutting mapping. Hill cutting activities over the past twenty years are

shown in red color (Figure 3b). Distance to the hill cutting is considered as a significant factor for landslides in CMA with an assumption – the likelihood of landslides is higher nearer to hill cutting areas.

### 2.4 Other landslide causative factors

Altitude zones, slope angle, slope aspect, geological unit, soil permeability, land cover, and distance to fault, road cut, stream, and drainage network were identified as other landslide causative factors. Fault and lineament, soil permeability, and surface geology layers were collected from the Geological Survey of Bangladesh. A Soil permeability map was classified with five different ordinal classes based on infiltration capacity – rapid, mixed moderate, moderate, slow, and very slow (Figure 4a). A surface geology map (Figure 4b) was classified into six nominal classes namely beach and dune sand, Boka bill formation, Dhing Formation, Dupi Tila formation, Tipam sand stone, and valley alluvium and colluvium. A land

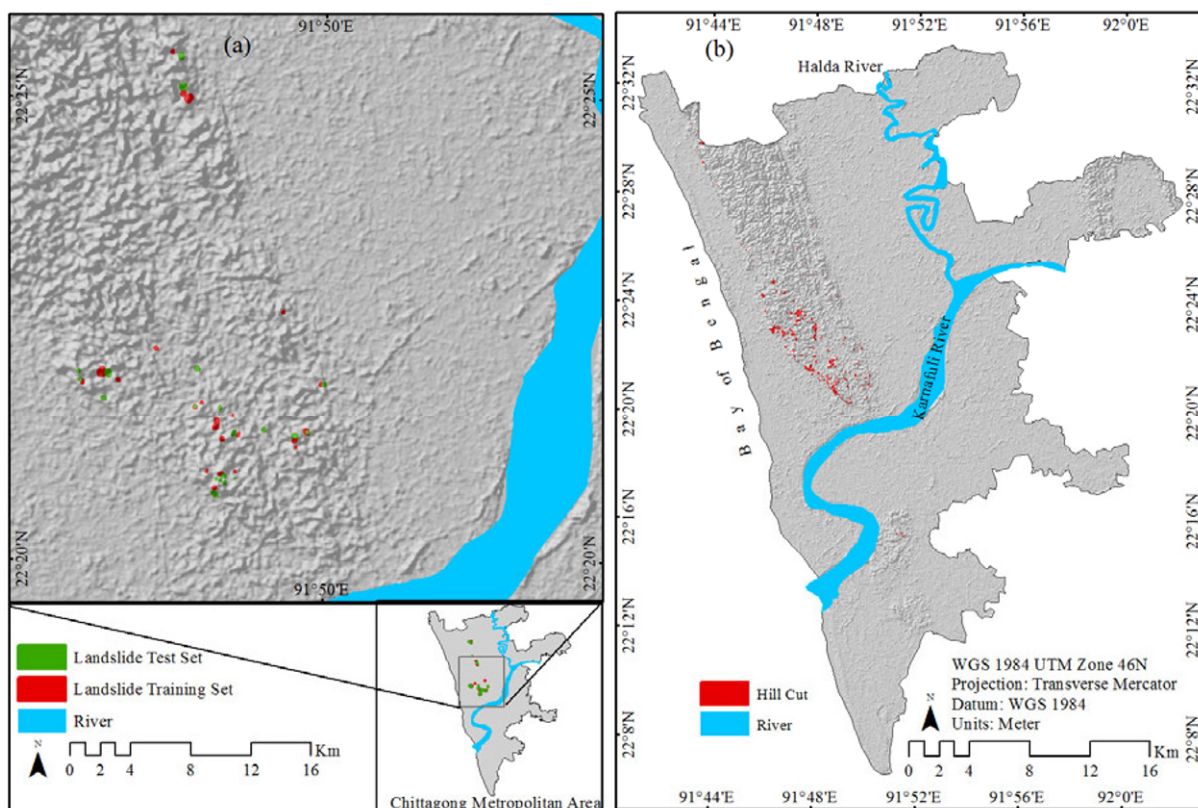


**Figure 3** (a) Landslide inventory map, and (b) hill cutting map of Chittagong Metropolitan Area (CMA) (1990-2010).

cover map (Figure 4c) with six distinctive classes was prepared from 2010 Landsat satellite image. The land cover map was validated using a Chittagong city guide map collected from CDA (Ahmed and Ahmed 2012; Ahmed 2015a).

A DEM image (dated 29 November 2013) was extracted from the Advanced Spaceborne Thermal Emission and Reflection Radiometer-Global Digital Elevation Model (ASTER-GDEM) web-portal. The ASTER-DEM image was used to produce altitude (Figure 5a) and slope map (Figure 5b). An aspect map is also generated from DEM that is a major factor for landslides because surface oriented to the sun is dried out easily after rain events. In general, aspect is the horizontal orientation of the surface

and represents the direction of a slope. The aspect map of CMA was divided into standard eight directional orientations (Figure 5c).

Landslides in CMA are also influenced by factors such as distance to existing drainage (Figure 6a), road cut (Figure 6b), stream network (Figure 6c), hill cut (Figure 7a), and fault line (Figure 7b). Distances to these linear features are either proportionally or inversely related to landslide susceptibility. The distance was calculated using the Euclidian distance technique. A daily-observed precipitation data (1960–2010) collected from the Bangladesh Meteorological Department (BMD) was used to prepare the average annual precipitation map (Figure 7c).

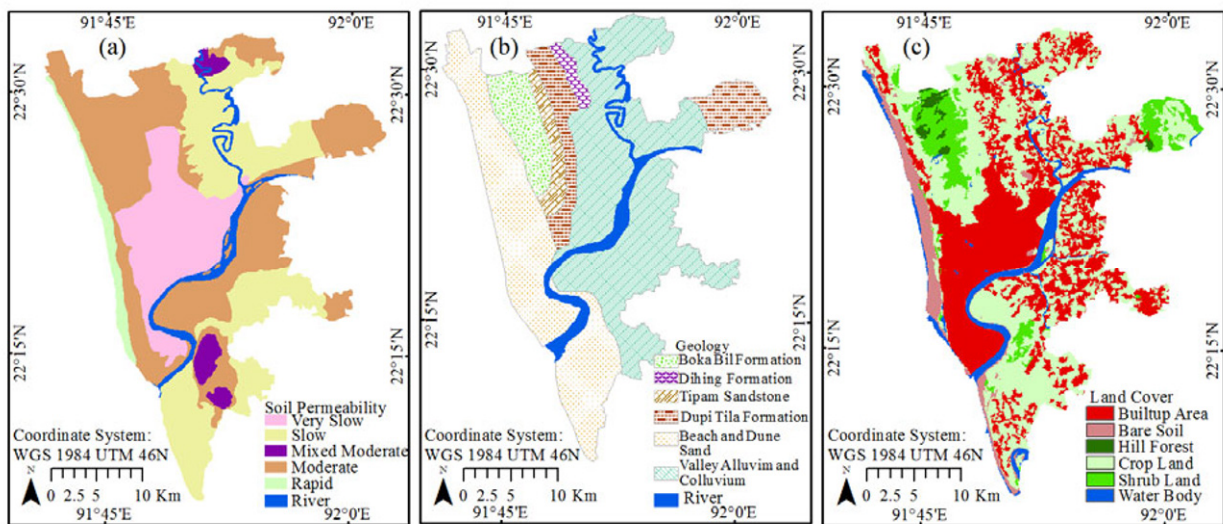


Figure 4 (a) Soil permeability, (b) surface geology, and (c) land cover map of Chittagong Metropolitan Area (CMA).

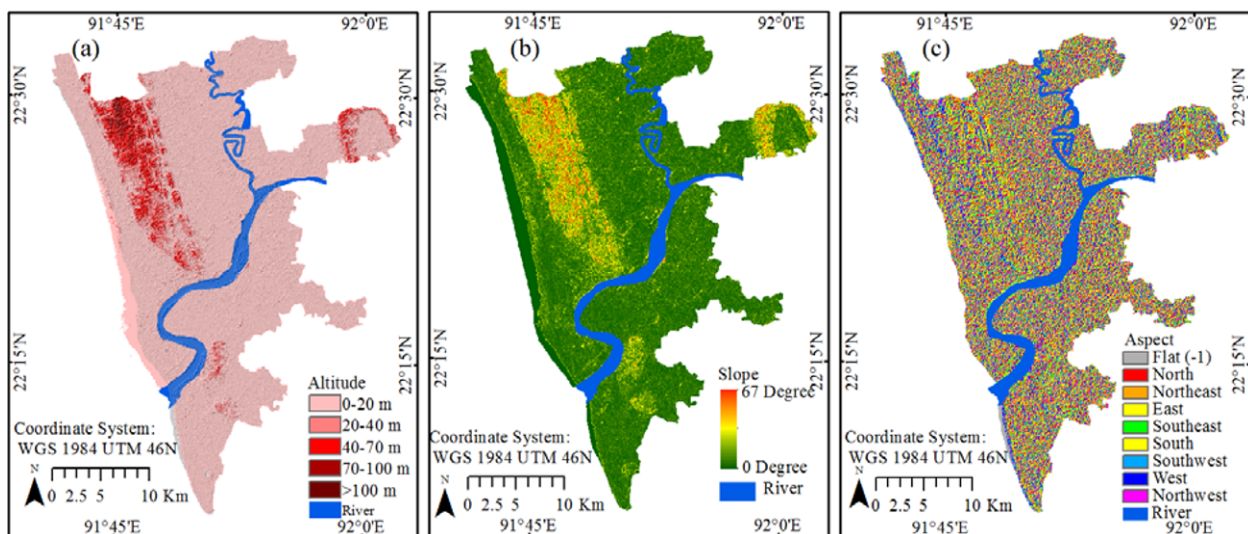


Figure 5 (a) Altitude, (b) slope, and (c) aspect map of Chittagong Metropolitan Area.

### 2.5 Landslide susceptibility modeling

Both knowledge driven spatial multi-criteria evaluation and data driven bivariate statistical methods were applied for landslide initiation modeling. An empirical runout modeling was applied to determine the susceptible area to runout.

#### 2.5.1 Conditional independence test

In the case of weights of evidence (WoE) modeling the application of conditional independence (CI) test is a prerequisite (Torizin 2016; Bonham-Carter 1994). It confirms the CI of

the dependent variables (Vijith et al. 2014). CI can be calculated using techniques such as chi-square test, Omnibus test, and new Omnibus test (Agterberg and Cheng 2002), etc. In this study, CI is evaluated by a pair-wise Cramer’s V that is a post-test to determine the strengths of the association after chi-square test has determined the significance (Cramér 1999). A chi-square test estimates whether there is any significant relationship between two variables (i.e. factor maps), but it does not tell the level of significance. Cramer’s V gives the information where the coefficient values range from 0 (small association) to 1 (strong association).

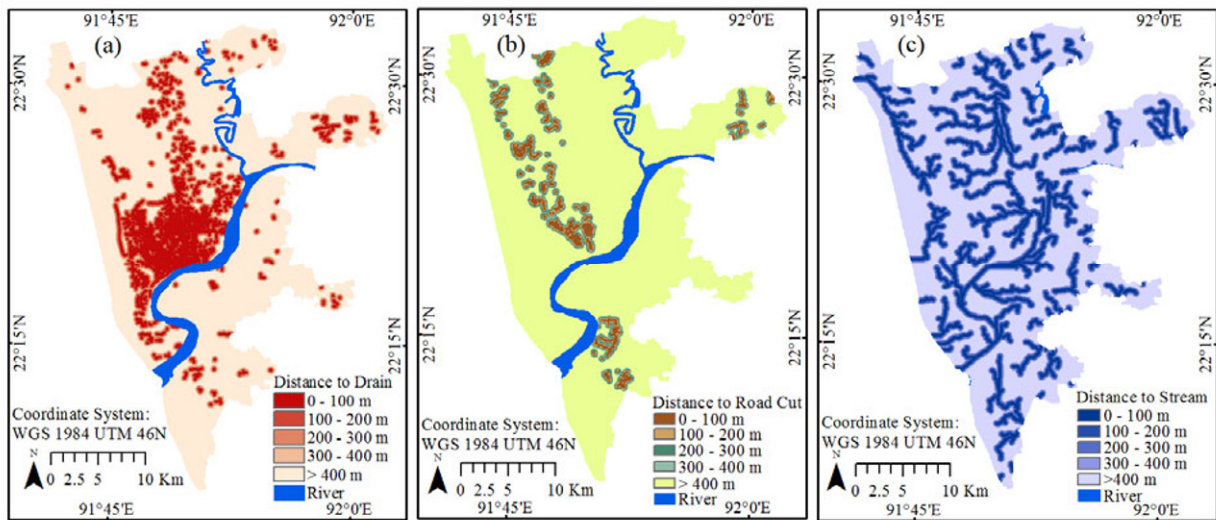


**Figure 6** Distance to (a) drainage network, (b) road cut, and (c) stream network map of Chittagong Metropolitan Area.

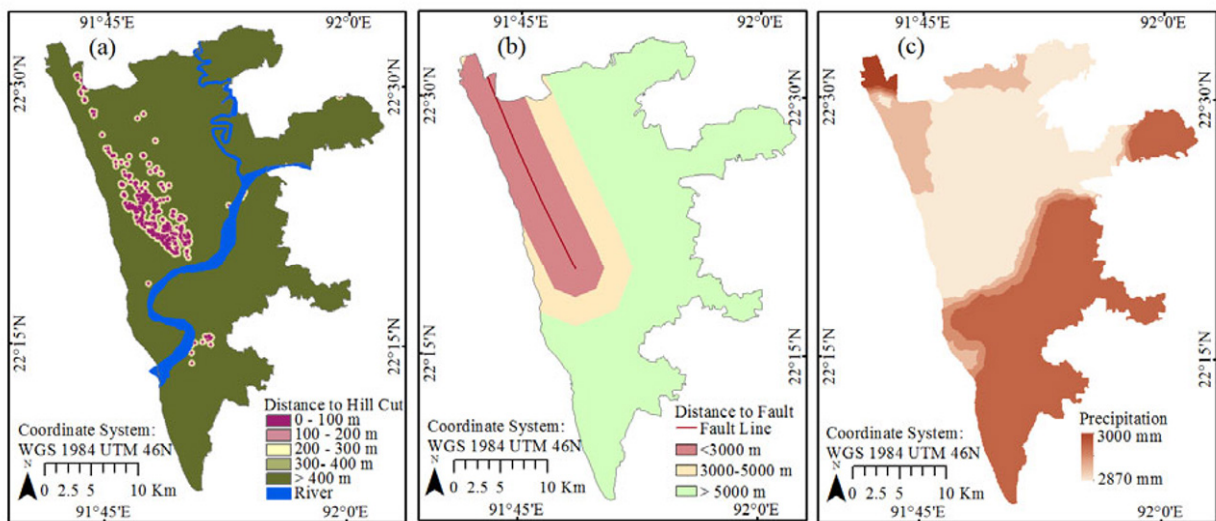


**Figure 7** (a) Distance to hill cut and (b) fault, and (c) average annual precipitation map of Chittagong Metropolitan Area.



### 2.5.2 Landslide initiation susceptibility modeling

#### (a) Weights of evidence (WoE)

Landslides in a particular geographical context are influenced by various geological, topographical and hydrological factors, etc. These factors need to be analyzed for identifying the possible areas that can be affected by landslides. Field experience and expert opinion are necessary to model landslide susceptibility for the knowledge driven approach. Results from data driven approach such as WoE can be a good indicator to put rational weights for these factors (Kayastha et al. 2012). The presence or absence of some factors might be favorable for landslides. Bayesian probability methods were proved to be effective in evaluating the importance of both presence and absence of a factor. The detail of the WoE method used in the article is explained in Bonham-Carter (1994). This process converts all the factor maps to weight maps. The landslide susceptibility score map was calculated by the arithmetic sum of all weight maps. The score map was classified into three classes – low, moderate, and high susceptibility based on the histogram analysis of the weight map.

#### (b) Analytical hierarchical process (AHP)

AHP is a technique to make decisions concerning a particular goal. AHP method is applied to derive the weights associated with attribute map layers (Saaty 1977; Kayastha et al. 2013). AHP builds a hierarchy of decision criteria through pairwise comparison of each possible criterion pair. The details of AHP method used in this article is described in Saaty (1977) and Saaty (1980).

Factor maps that are influential for triggering landslides were considered for LSM. These factor maps were grouped, standardized and weighted in a criteria tree. The factor maps were then given weights based on the importance of factor classes related to landslide occurrence. Expert opinion was used as a guideline for incorporating AHP and fuzzy logic (Zimmermann 1991; Bonham-Carter 1994; Malczewski 2004). Fuzzy weights from 0 to 1 were assigned (Eastman 2012). After the standardization process, the first level of weights was assigned for each factor map from the broad factor groups. The second tier of weights was given

based on the qualitative judgment of the importance of the landslide causative factors.

In this study, all factor maps were grouped into five categories - hydrology, geology, topography, topography alteration, and land cover. Soil permeability, precipitation, distance to drainage and distance to streams were grouped as hydrological factors. Slope and aspect layers were considered as topographic factors. Distance to hill cut and road cut were considered as topographic alteration factors.

### 2.5.3 Landslide runout modeling

The runout modeling is the calculation of the spreading of the initiated failed mass. The location of a landslide initiation was calculated from the initiation susceptibility. The highest 5% of the initiation susceptible areas were considered (for maintaining higher accuracy and reliability) as a source of landslide initiation in runout modeling. The model used in this study was developed at the University of Lausanne, Switzerland, called Flow-R (Horton et al. 2013). The runout estimation is based on the probabilistic and energy calculation, which allows identifying the runout of the landslide from the initiation sources. The DEM and landslide initiation source maps were the inputs of the model to calculate landslide propagation based on the frictional laws and flow direction algorithms (Horton et al. 2013). The flow direction was calculated based on the modified Holmgren's algorithm by changing the height of the central cell by a factor  $dh$ , which will change the gradients values (Holmgren 1994).

### 2.5.4 Combined LSM and model validation

The consistency of LSM was tested by landslide density, relative operating characteristic (ROC) curve and spatially agreed on area analysis techniques (Kayastha et al. 2013; Bijukchhen et al. 2013). ROC analysis is useful for cases where it is possible to see how well the suitability map portrays the location of a particular category. The minimum value of an area under ROC curve (AUC) is 0.5, which means no improvement over the random assignment. The maximum value of AUC is 1 that denotes perfect discrimination (Eastman 2012). The step-by-step methodological flowchart is illustrated in Figure 8.

In summary, initially, twelve landslide causative factor maps were prepared to represent the context and nature of landslides in CMA. As independence of the factors is required for the WoE modeling, a conditional independence test was applied. The dependent factors were excluded from the subsequent analysis. In the next step, the landslide-training map was overlaid with the 10 CI passed factor maps to calculate the positive and negative weights, and contrast factors. The factor weight maps were prepared from the weight tables. All the weight maps were then combined to get the WoE susceptibility score map. The AHP susceptibility score map was prepared to apply the spatial multi-criteria decision-making tree. The experts gave the weights of importance for the AHP pairwise comparison.

Both the susceptibility score maps were then converted to LSM based on the histogram characteristics and the cumulative function of the score. Top 5% score of the AHP susceptibility map was used as the landslide initiation source for the runout modeling. AHP LSM was chosen over WoE based on higher ROC value. The runout susceptibility was then converted to runout susceptibility class map. The AHP generated initiation, and runout susceptibility maps were incorporated to prepare the combined LSM.

### 3 Results and Discussion

#### 3.1 Results from CI test

The Cramer's V ratio calculated for all the possible pairs of the selected dependent variables are given in [Table 1](#). The Cramer's V coefficient values  $>0.5$  represents that the two variables are highly associated ([Crewson 2016](#)). In this case, the distance to fault and altitude maps showed Cramer's V values  $>0.5$  ([Table 1](#)). Consequently, these two variables were excluded from further analysis as they are showing conditional dependence with other variables.

#### 3.2 Results from WoE

The importance of factor classes and contrast

factors are summarized in [Appendix 1](#). The positive contrast factor ( $C_w$ ) indicates that there is a positive association between two variables (bivariate); i.e. the factor class and landslides. The negative contrast factor shows that there is a negative association between the factor class and landslides. WoE results show ([Appendix 1](#)) that most of the landslides fall in the precipitation class 2870–2880 mm/year. CMA falls within 2870–3000 mm annual rainfall range ([Figure 7c](#)), where the overall variation of rainfall is negligible on a local scale. Still, the precipitation map is considered for analysis, as the landslides in CMA are mostly associated with monsoon rainfall ([Ahmed 2015a](#)).

North, northeast, west, south, and southwest aspect classes show positive contrast, which is highly associated with landslide occurrences as per data driven results. However, from the sun exposure perspective south-facing slope is more exposed to the sun and the north-facing slope is least exposed to the sun. North aspect is the most and south aspect is the least susceptible to landslides. Moving from south to north in both directions should gradually become more vulnerable to landslides. These aspects are covered by shades that take longer durations to dry out after consecutive days of rainfall. Middle slope zones were found more susceptible than the other slope conditions because people do not prefer to build houses at hilltops. Areas closer to hill cut, road cut and existing drainage network were found more susceptible to landslides, as these areas are vulnerable to landslides. The opposite result is found in the case of stream network – areas far from stream network were found more favorable for landslide occurrence (positive contrast) than areas closer to stream (negative contrast). Very low soil permeability class shows a higher positive contrast (8.31) as it fails to absorb and infiltrate surface runoff quickly. Dupi Tila (1.33) and Tipam sandstone (3.55) surface geological classes have positive contrast factor values indicating that these two geological classes are favorable for landslides. Built up area class shows a positive (1.26) contrast ([Appendix 1](#)). In CMA, most landslides occur in areas where residential housing has been constructed by cutting hills or disrupting the natural slope ([BUET-JIDPUS 2015](#)).

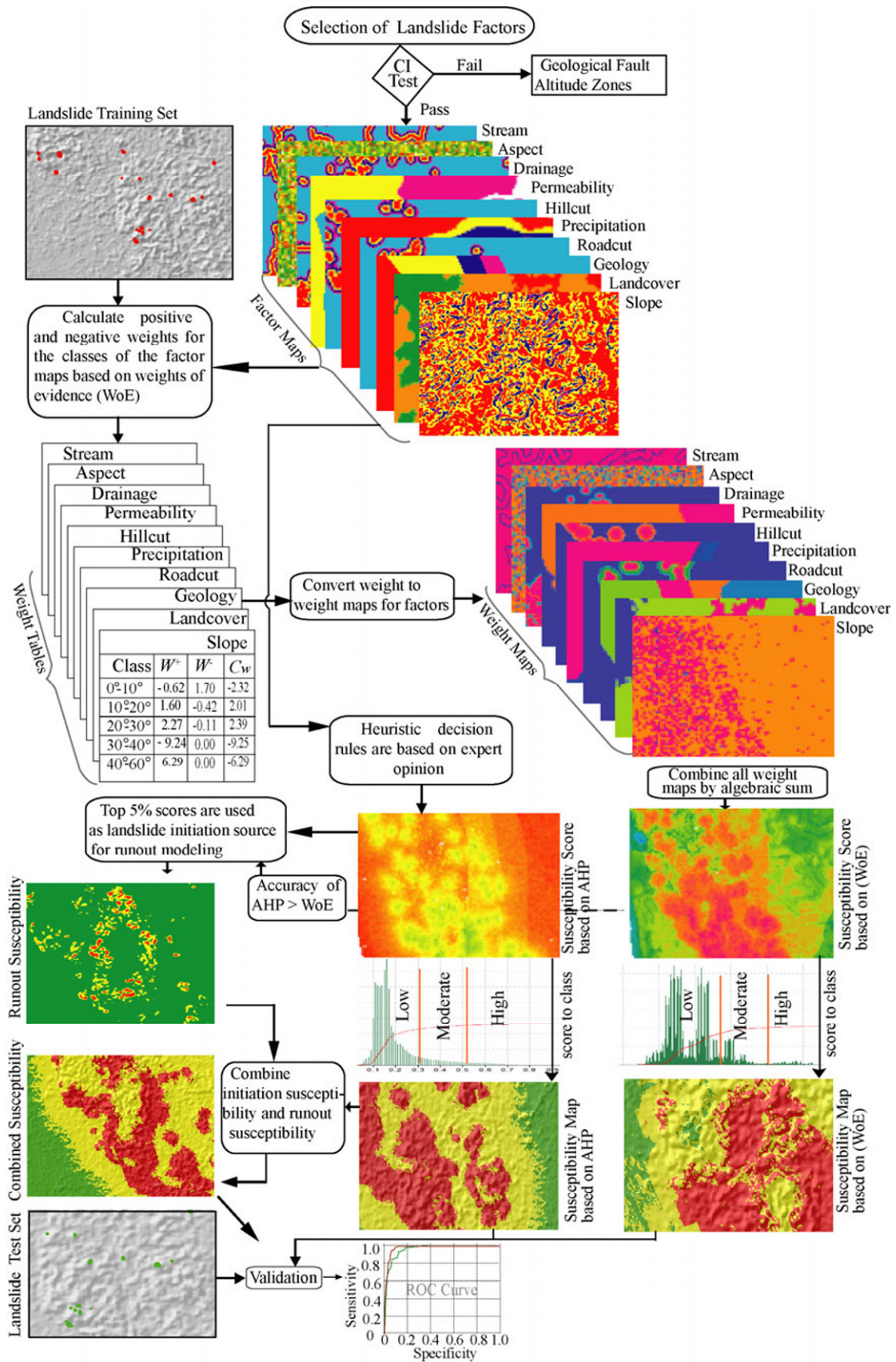


Figure 8 Methodological flowchart of the study.

**Table 1** Pair-wise conditional independence (CI) test values for Cramer’s V

Variables	1	2	3	4	5	6	7	8	9	10	11	12
Altitude (1)	-	0.44	0.44	0.62	0.56	0.48	0.54	0.48	0.51	0.45	0.44	0.44
Aspect (2)	-	-	0.45	0.58	0.41	0.45	0.40	0.44	0.50	0.43	0.44	0.44
Drain (3)	-	-	-	0.60	0.47	0.46	0.48	0.45	0.44	0.39	0.44	0.46
Fault (4)	-	-	-	-	0.69	0.62	0.60	0.59	0.59	0.65	0.57	0.65
Geology (5)	-	-	-	-	-	0.47	0.49	0.47	0.45	0.49	0.44	0.48
Hill cut (6)	-	-	-	-	-	-	0.44	0.50	0.45	0.45	0.44	0.45
Land cover (7)	-	-	-	-	-	-	-	0.45	0.48	0.50	0.45	0.46
Road (8)	-	-	-	-	-	-	-	-	0.45	0.45	0.44	0.44
Slope (9)	-	-	-	-	-	-	-	-	-	0.44	0.45	0.44
Soil (10)	-	-	-	-	-	-	-	-	-	-	0.43	0.47
Stream (11)	-	-	-	-	-	-	-	-	-	-	-	0.44
Rainfall (12)	-	-	-	-	-	-	-	-	-	-	-	-

### 3.3 Results from AHP

The importance of the classes in each causative factor map is standardized by the fuzzy membership (Zimmermann 1991; Ahmed and Ahmed 2012). A discrete fuzzy membership value (from 0 to 1) for each categorical variable is given based on the local context and association with landslides, and expert opinion. It is observed that the probability of landslides increases with the decrease of distances to road cut and hill cut factors. In the case of the two hydrological factors - far from streams and closer to drainage network were found to be favorable for landslides. Consequently, a fuzzy membership value of 1 is assigned for the nearest distance to hill cut, road cut, and drainage (Appendix 2). The membership value is gradually decreased with the distance to these three factors and becomes zero at 400 m (where there is no influence for landslide occurrences). The areas closer to stream network is less favorable for landslides. A gradually increasing fuzzy membership value from 0–1 is assigned to the cells with values from 0–400 m for the distance to stream factor map (Appendix 2). The middle slope zone is found highly vulnerable to landslides. It is not possible to build houses on very steep slopes, and houses located in the foothill are comparatively less vulnerable. Consequently, the middle slope zones are assigned with the highest fuzzy membership value, and lower weights are assigned for both the gentle and steep slopes (Appendix 2). A fuzzy weight of 0.4 is assigned for the ‘2870–2880 mm/year’ precipitation zone, and then the membership value is increased to 1 for the precipitation class ‘3000 mm/year’ (Appendix 2). The north-facing slopes (aspect) are highly, and the

south facing slopes are less favorable to landslides (Robinson and Brown 2009). The fuzzy membership values are assigned accordingly (Appendix 2). Tipam and Dupi Tila formations are comprised of loose and less resistive sandstone layers and are accountable for maximum landslides (Ahmed and Rubel 2013). A full membership weight (1.0) is assigned to Tipam sandstone geological unit, and half membership weight (0.5) is assigned to Dupi Tila formation unit. Urban built-up areas are highly vulnerable to landslides as hill cutting for developing settlements are common in those areas. Fuzzy membership weights of 1, 0.8, and 0.6 are assigned to urban built-up areas, cropland, and shrub land respectively. Very slow, slow, and moderate soil permeability classes are respectively assigned with 1, 0.6, and 0.4 factor weights (Appendix 2).

In the next stage, AHP pairwise comparison is applied to the factor maps. All the factor maps are initially grouped into five broad categories. To begin with, the eigenvalues and associated expert weights for the hydrological factor maps are shown in Table 2. It is obtained by setting the following criteria – permeability is moderately less important than drainage, permeability is moderately more important than a stream, permeability is strongly more important than precipitation, drainage is strongly more important than a stream, drainage is very strongly more important than rainfall, and the stream is moderately more important than rainfall. The overall consistency ratio for the hydrological factors is found to be 0.04 (Table 2). It indicates that the AHP analysis is statistically acceptable (Saaty 1977; Ahmed 2015a). Like the hydrological factors, AHP pairwise comparison has also been applied to topographic factors and topographic

alteration factors (Table 3 and Table 4). Aspect is considered as moderately less important than slope within topographic factors. Hill cut is considered as moderately more important than road cut within topographic alteration factors. Since there are only two factors in both topographic and topographic alteration group; there is no possibility of inconsistency. The pairwise comparison is not required for land cover and geology factors, as they do not belong to any specific group.

An AHP pairwise comparison is also conducted among the five broad categories (Table 5) that are given the name 'first level criteria.' For the first tier, the groups are given weights based on the subjective judgment of the importance for triggering landslides. The judgments are per se - hydrology and geology are equally important, hydrology is moderately less important than topography, hydrology is strongly less important than topography alteration, hydrology is strongly more important than the land cover, and so on (Table 5).

The AHP weighting is finally summarized into two weight groups: first and second level criteria (Table 6) based on Tables 2-5. The first group is associated with the broad five-factor groups (i.e. first level criteria), and the second group is linked to the relevant factors (i.e. second level criteria). In the AHP susceptibility analysis, values of each class

**Table 2** Pairwise comparison matrix and factor weights for the hydrological factors

Factors	Soil permeability	D1	D2	Precipitation	Eigen values
Soil permeability	1	1/3	3	5	0.262
D1		1	5	7	0.565
D2			1	3	0.118
Precipitation				1	0.055
Inconsistency ratio: 0.041 (acceptable)					

**Notes:** D1=Distance to drainage; D2=Distance to streams.

**Table 3** Pairwise comparison matrix and weights for the topographic factors

Topographic factors	Aspect	Slope	Weights
Aspect	1	1/3	0.25
Slope		1	0.75

**Table 4** Pairwise comparison matrix and weights for the topographic alteration factors

Factors	Hill cut	Road cut	Weights
Hill cut	1	3	0.75
Road cut		1	0.25

of causative factors are taken from fuzzy membership, and then the factors are weighted in two levels.

### 3.4 Landslide initiation susceptibility mapping

At this stage, the positive and negative weights were calculated (Appendix 1) to produce the weight maps. The WoE based landslide susceptibility score map was then prepared by applying the arithmetic sum of the weight maps (Appendix 3a). The AHP susceptibility score map (Appendix 3b) is prepared by a spatial multicriteria analysis based on the given importance from the expert point of view. Both the WoE and AHP score maps were then classified into three susceptibility classes: low, moderate, and high by analyzing the histogram natural break and cumulative curve. Four modes were found in the WoE histogram distribution (Appendix 4a). Since the target is to classify susceptibility score maps in three nominal categories, the first two modal groups were categorized as low susceptibility at 5.32 cutoff score that covers 75% of the study area. The cumulative distribution also aided this classification. 75%, 20%, and 5% areas respectively were classified as low, moderate and high susceptible zones for WoE (Appendix 4a). For the AHP LSM, the cutoff values for the 'low to moderate' and 'moderate to high' susceptibility classes were chosen as 0.167 and 0.46, respectively (Appendix 4b). Similar percentages of areas were classified for susceptibility zoning. By this way, the susceptibility score maps were converted to prepare the WoE (Figure 9a) and AHP landslide initiation susceptibility maps (Figure 9b).

### 3.5 Combined susceptibility mapping

The energy travel angle was set to 15° and energy initiation velocity was set to 15 m/s (Van Westen et al. 2014) for landslide runout modeling. After calculating the runout susceptibility scores, the runout susceptibility map was prepared (Figure 10a). The runout susceptibility map and AHP LSM were combined (as AHP AUC > WoE AUC). The combined LSM was classified into three nominal classes: low, moderate, and high susceptible zone (Figure 10b). The presence of low susceptibility in

**Table 5** Pairwise comparison matrix and factor weights for the group/ first level factors

First tier criteria	Hydrology	Geology	Topography	Topography alteration	Land cover	Weights
Hydrology	1	1	1/3	1/5	3	0.100
Geology		1	1/3	1/5	5	0.116
Topography			1	1/3	5	0.243
Topography alteration				1	7	0.498
Land cover					1	0.042

Inconsistency ratio: 0.046 (acceptable)

**Table 6** Summary of weights from analytical hierarchical process (AHP) analysis

First level criteria	Second level criteria	Second level weight	First level weight
Hydrological factors	Soil permeability	0.262	0.100
	Distance to drainage	0.565	
	Distance to stream	0.118	
	Precipitation	0.055	
Geological factor	Surface geology	1.000	0.116
Topographic factors	Aspect	0.250	0.243
	Slope	0.750	
Topography alteration factors	Distance to hill cut	0.750	0.499
	Distance to road cut	0.250	
Land cover	Land cover	1.000	0.042

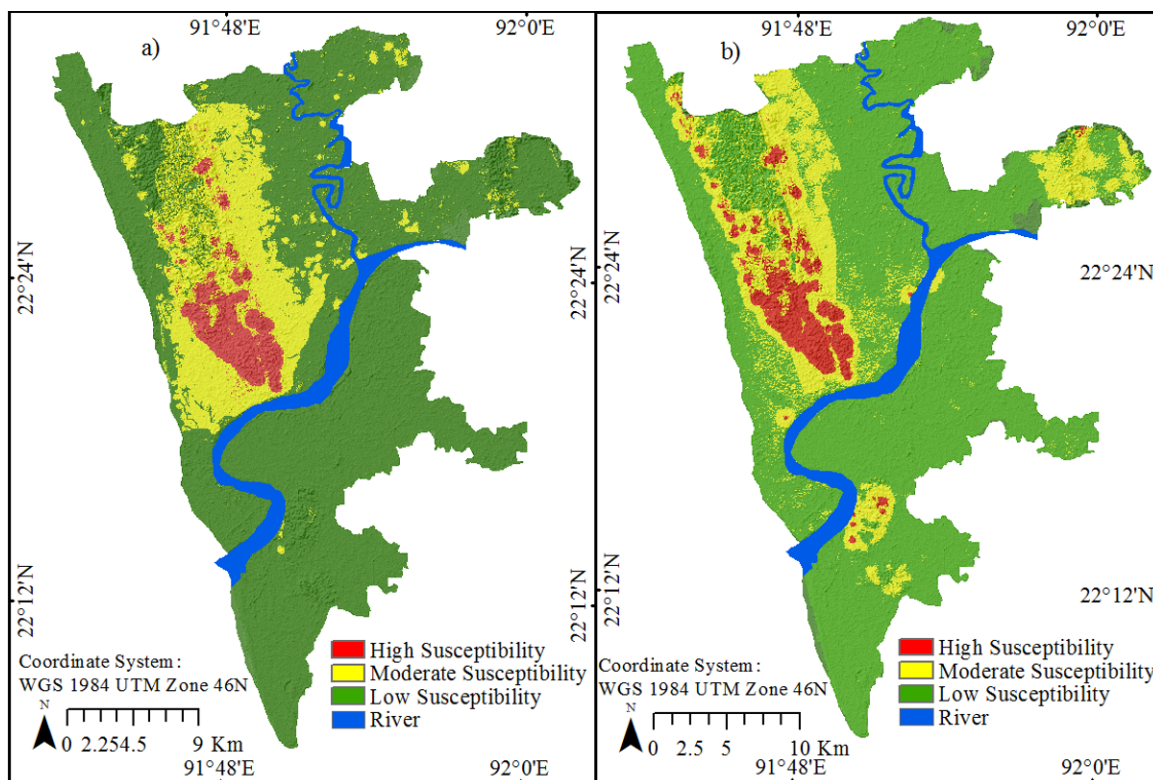


**Figure 9** Landslide initiation susceptibility map based on (a) WoE, and (b) AHP.

both susceptible maps was considered as low, high susceptibility in any map was considered as high, and remaining areas were considered as moderate susceptible zone (Appendix 5). The higher 5% areas of the AHP landslide initiation susceptibility score

was selected for the landslide runout modeling. The combined landslide susceptibility map (Figure 10b) was validated using the testing landslide locations (Figure 3a) and by applying the ROC method (Eastman 2012).

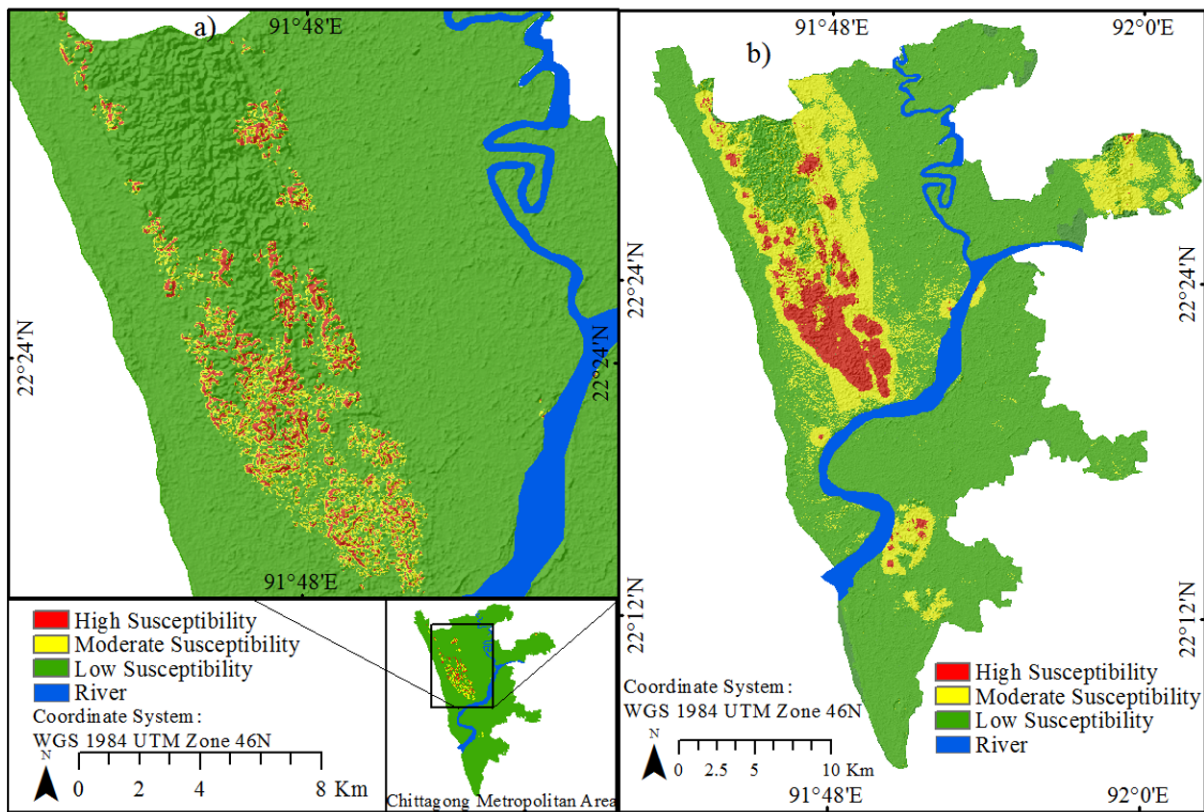


**Figure 10** (a) Landslide runout susceptibility interest zones, and (b) combined (initiation and runout) landslide susceptibility map of CMA.

### 3.6 Model validation and consistency analysis

Figure 11 illustrates the validation results obtained from the ROC curve. The red line is indicating the prediction rate (i.e. validated by training landslides) and the green line indicates the success rate (i.e. validated by testing landslides). The higher accuracy of a success rate indicates the higher accuracy and better performance of a model. The accuracy of WoE, AHP, and combined LSM was calculated respectively as 96%, 97%, and 98% indicating a gradual improvement in modeling outcome (Figure 11).

The high susceptibility zone should have the highest landslide density, sequentially decreased for the medium and low susceptibility zones. This is the general theory of landslide density calculation (Kayastha et al. 2013; Bijukchhen et al. 2013). A total of 5%, 20%, and 75% areas were categorized as high, moderate, and low susceptible (Table 7). The percentages of landslide areas were found to be highest for the high susceptibility zone

(82%–85%) followed by the medium (15%–17%) and low zones (<1%). This trend was also similar for the landslide density for the three different susceptibility zones. The total density (0.0002) and zone-wise density pattern were also found consistent for all the LSMs (Table 7). It authenticates that the three different LSMs as produced in this study are quantitatively similar.

The spatially agreed areas between the two landslide susceptibility maps were calculated to understand the overall performance (Appendix 6). In the case of the WoE and AHP, and WoE and combined approximately 82% areas fell in identical susceptibility zones. The statistic was found higher (99%) for the AHP and combined LSMs. For the WoE and AHP comparison, 91% landslides were found in the agreed areas, of which 78% landslides were found in the agreed high susceptibility zone that covers around 4% of the study area. The AHP and combined methods presented highest agreement (around 96%), of which 80% landslides were found in high susceptible zone covering around 5% of the total area (Appendix 6). It proves that the predicted LSMs have high spatial

agreement (Kayastha et al. 2013; Bijukchhen et al. 2013).

Based on the model validation results, it is affirmed that the LSMs as produced in this study are statistically consistent and identical, showing higher level of performance, and are scientifically valid. The datasets were mostly collected from the concerned public organizations in Bangladesh. A 30m resolution DEM, and Landsat satellite images were used for analysis. It is admitted that the availability of higher resolution satellite images, improved datasets, additional resources and intense fieldwork for landslide inventory preparation, and sufficient ground-truth activities to deal with the uncertainties in weight valuation process could improve the overall results and reduce the existing minimal level of inconsistencies.

#### 4 Conclusions

Rainfall induced landslides are gradually becoming a matter of serious concern for the communities living in the mountainous or hilly areas worldwide. The Chittagong hill districts are also highly vulnerable to landslides and associated flash flooding. Rapid urbanization, indiscriminate hill cutting and deforestation, global warming and lack of cultural/indigenous knowledge to deal with the hilly environment are aggravating landslide disasters. This scenario is evident in CMA. The aim of this research was to prepare a reliable and scientifically valid landslide susceptibility map to foster the landslide DRR activities.

Ten-factor maps – land cover, slope, altitude, soil permeability, surface geology, hill cutting,

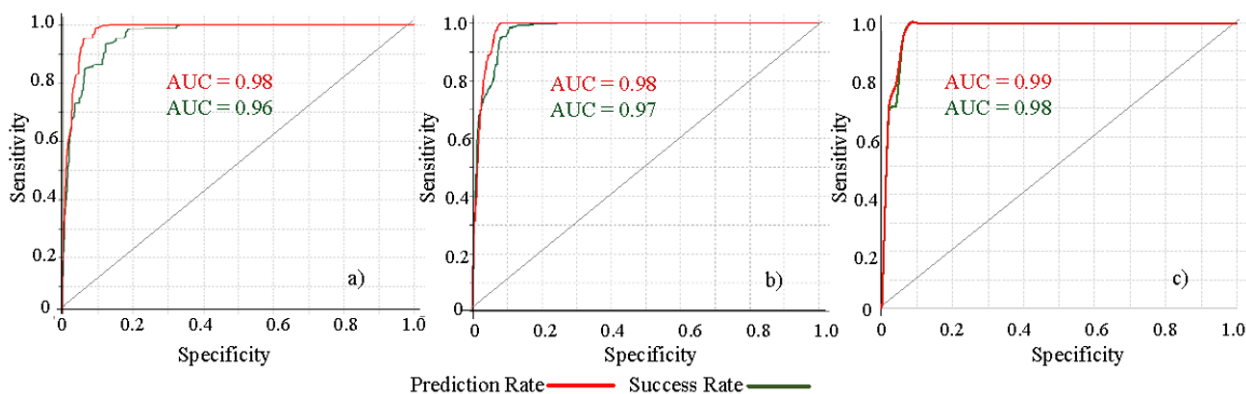


Figure 11 ROC curves for (a) weights of evidence, (b) AHP, and (c) combined map.

Table 7 Landslide density calculation for different susceptibility maps

Methods		Susceptibility zones			
		Low	Moderate	High	Total
Weights of Evidence (WoE)	Area (km <sup>2</sup> )	505.4	134.73	33.8	673.93
	Area (%)	75	20	5	100.00
	Landslide area (km <sup>2</sup> )	0.0011	0.029	0.1366	0.1667
	Landslide area (%)	0.66	17.40	81.94	100.00
	Landslide density	0.000002	0.00022	0.00404	0.0002
Analytic Hierarchy Process (AHP)	Area (km <sup>2</sup> )	505.07	135.02	33.84	673.93
	Area (%)	75	20	5	100.00
	Landslide area (km <sup>2</sup> )	0.00020	0.0287	0.1378	0.1667
	Landslide area (%)	0.12	17.22	82.66	100.00
	Landslide density	0.0000004	0.00021	0.00407	0.0002
Combine (AHP and Runout)	Area (km <sup>2</sup> )	505.06	133.56	35.31	673.93
	Area (%)	75	20	5	100.00
	Landslide area (km <sup>2</sup> )	0.0006	0.0252	0.1409	0.1667
	Landslide area (%)	0.36	15.12	84.52	100.00
	Landslide density	0.0000012	0.0001887	0.0040	0.0002



aspect, distance to existing drainage network, faults, road cut and stream network – were selected based on CI test. A WoE method was applied to calculate the positive (presence of landslides) and negative (absence of landslides) factor weights. Then a combination of AHP and fuzzy membership standardization (weights from 0 to 1) was implemented. The Flow-R tool, which allows to model landslide runoff from the initiation sources, was applied. The flow direction was calculated using the modified Holmgren's algorithm. The methods were chosen based on applicability in this particular context. The AHP initiation and runoff susceptibility maps were combined for preparing the final landslide susceptibility map. The ROC curve was used for model validation purpose. A total of 5%, 20%, and 75% areas were respectively

categorized as high, moderate, and low landslide susceptible zone.

It is highly recommended to incorporate landslide susceptibility maps in existing master plans for a city like Chittagong that is surrounded by hills and dominated by highly marginalized communities. The outcome of this research would be helpful for the urban planners and concerned stakeholders to restrict the unplanned housing development in landslide prone areas. It can also facilitate to prepare necessary emergency and risk sensitive land use plans, developing a Web-GIS based landslide early warning system, and to assist reducing the impacts of landslide disasters in Chittagong Metropolitan Area and other similar hilly communities in Bangladesh.

## Acknowledgement

Md. Shahinoor Rahman is funded by the Center for Spatial Information Science and Systems at George Mason University, USA. Bayes Ahmed is a Commonwealth Scholar funded by the UK govt. We are grateful to the Chittagong Development Authority, Geological Survey of Bangladesh, Chittagong City Corporation, Bangladesh Meteorological Department, Survey of Bangladesh, Bangladesh Agricultural Research Council, U.S. Geological Survey, and the National Aeronautics and Space Administration for providing the necessary datasets. We want to thank

the field remunerators and the local people for their unconditional support. Finally, our profound gratitude goes to the editors of the Journal of Mountain Science and the three anonymous reviewers for their insightful comments that contributed to improve the quality of the manuscript.

**Electronic Supplementary Material:** Supplementary material (Appendixes 1-6) is available in the online version of this article at <https://doi.org/10.1007/s11629-016-4220-z>.

## References

- Agterberg FP, Cheng Q (2002) Conditional independence test for weights-of-evidence modeling. *Natural Resources Research* 11(4): 249-255. <https://doi.org/10.1023/A:1021193827501>
- Ahmed B (2015a) Landslide susceptibility mapping using multi-criteria evaluation techniques in Chittagong Metropolitan Area, Bangladesh. *Landslides* 12(6): 1077-1095. <https://doi.org/10.1007/s10346-014-0521-x>
- Ahmed B (2015b) Landslide susceptibility modelling applying user-defined weighting and data-driven statistical techniques in Cox's Bazar Municipality, Bangladesh. *Natural Hazards* 79(3): 1707-1737. <https://doi.org/10.1007/s11069-015-1922-4>
- Ahmed B, Dewan A (2017) Application of bivariate and multivariate statistical techniques in landslide susceptibility modeling in Chittagong City Corporation, Bangladesh. *Remote Sensing* 9(4): 304. <https://doi.org/10.3390/rs9040304>
- Ahmed B, Kamruzzaman M, Zhu X, et al. (2013) Simulating land cover changes and their impacts on land surface temperature in Dhaka, Bangladesh. *Remote Sensing* 5(11): 5969-5998. <https://doi.org/10.3390/rs5115969>
- Ahmed B, Ahmed R (2012) Modeling urban land cover growth dynamics using multi-temporal satellite images: a case study of Dhaka, Bangladesh. *ISPRS International Journal of Geo-Information* 1(1): 3-31. <https://doi.org/10.3390/ijgi1010003>
- Ahmed B, Rahman MS, Rahman S, et al. (2014) Landslide inventory report of Chittagong Metropolitan Area, Bangladesh. BUET-Japan Institute of Disaster Prevention and Urban Safety (BUET-JIDPUS), Bangladesh University of Engineering and Technology (BUET), Dhaka, Bangladesh. <https://www.landslidebd.com> (accessed on 19 December 2016)
- Ahmed B, Rubel YA (2013) Understanding the issues involved in urban landslide vulnerability in Chittagong metropolitan area, Bangladesh. *Association of American Geographers*

- (AAG), Washington DC, USA. <https://sites.google.com/a/aag.org/mycoe-servirglobal/final-arafat> (accessed on 16 December 2016)
- Alexander DE (2000) Confronting catastrophe: new perspectives on natural disasters. Oxford University Press. p 290.
- Bai SB, Cheng C, Wang J, et al. (2013) Regional scale rainfall- and earthquake-triggered landslide susceptibility assessment in Wudu County, China. *Journal of Mountain Science* 10 (5): 743-753. <https://doi.org/10.1007/s11629-013-2432-z>
- BBS (2012). Community Report: Chittagong Zila. Population and housing census 2011, Bangladesh Bureau of Statistics (BBS), Ministry of Planning, Bangladesh. [http://203.112.218.65/WebTestApplication/userfiles/Image/PopCen2011/Com\\_Chittagong.pdf](http://203.112.218.65/WebTestApplication/userfiles/Image/PopCen2011/Com_Chittagong.pdf) (accessed on 19 October 2016)
- Beguiría S, Van Hees MJ, Geertsema M (2009) Comparison of three landslide runout models on the Turnoff Creek rock avalanche, British Columbia. *Landslide Process: from geomorphology mapping to dynamic modeling*. CERIG Edition, Strasbourg: 243-247. [https://www.researchgate.net/profile/Marten\\_Geertsema/publication/270893463\\_Comparison\\_of\\_three\\_landslide\\_runout\\_models\\_on\\_the\\_Turnoff\\_Creek\\_rock\\_avalanche\\_British\\_Columbia/links/54b842a20cf28face620784.pdf](https://www.researchgate.net/profile/Marten_Geertsema/publication/270893463_Comparison_of_three_landslide_runout_models_on_the_Turnoff_Creek_rock_avalanche_British_Columbia/links/54b842a20cf28face620784.pdf) (accessed on 10 November 2016)
- Berti M, Simoni A (2007) Prediction of debris flow inundation areas using empirical mobility relationships. *Geomorphology* 90(1): 144-161. <https://doi.org/10.1016/j.geomorph.2007.01.014>
- Bijukchhen SM, Kayastha P, Dhital MR (2013) A comparative evaluation of heuristic and bivariate statistical modelling for landslide susceptibility mappings in Ghurmi–Dhad Khola, east Nepal. *Arabian Journal of Geosciences* 6(8): 2727-2743. <https://doi.org/10.1007/s12517-012-0569-7>
- Bonham-Carter GF (1994) Geographic Information Systems for geoscientists-modeling with GIS. *Computer methods in the geoscientist* 13: 398.
- Bonham-Carter GF, Agterberg FP, Wright DF (2013) Integration of geological datasets for gold exploration in Nova Scotia. *Digital Geologic and Geographic Information System*, (American Geophysical Union). pp 15-23. <https://doi.org/10.1029/SC010p0015>
- Brunsdén D (1999) Some geomorphological considerations for the future development of landslide models. *Geomorphology* 30 (1): 13-24. [https://doi.org/10.1016/S0169-555X\(99\)00041-0](https://doi.org/10.1016/S0169-555X(99)00041-0)
- BUET-JIDPUS (2015) Developing a dynamic Web-GIS based early warning system for the communities living with landslide risks in Chittagong metropolitan area, Bangladesh. BUET-Japan Institute of Disaster Prevention and Urban Safety (BUET-JIDPUS), Bangladesh University of Engineering and Technology (BUET), Dhaka, Bangladesh. <https://www.landslidebd.com> (accessed on 19 November 2016)
- Chen H, Lee CF (2004) Geohazards of slope mass movement and its prevention in Hong Kong. *Engineering Geology* 76(1): 3-25. <https://doi.org/10.1016/j.enggeo.2004.06.003>
- Chisty KU (2014) Landslide in Chittagong City: A perspective on hill cutting. *Journal of Bangladesh Institute of Planners* 7: 1-17
- Couture R (2011) Landslide terminology-national technical guidelines and best practices on landslides. Geological Survey of Canada Open File 6824. <ftp://ftp.glf.c.forestry.ca/ess/GSC-landslide/of6824-ChapterB-Feb2011.pdf> (accessed on 17 October 2016)
- Cramér H (1999) *Mathematical Methods of Statistics*. Princeton University Press.
- Crewson P (2016) *Applied statistics: desktop reference*. First edition, AcaStat Software. Florida, USA. (<http://www.acastat.com/statbook/statbook.html> (accessed on 7 November 2016))
- Dai FC, Lee CF, Ngai YY (2002) Landslide risk assessment and management: an overview. *Engineering Geology* 64(1): 65-87. [https://doi.org/10.1016/S0013-7952\(01\)00093-X](https://doi.org/10.1016/S0013-7952(01)00093-X)
- Du GL, Zhang YS, Iqbal J, et al. (2017) Landslide susceptibility mapping using an integrated model of information value method and logistic regression in the Bailongjiang watershed, Gansu Province, China. *Journal of Mountain Science* 14 (2): 249-268. <https://doi.org/10.1007/s11629-016-4126-9>
- Eastman JR. (2012) IDRISI Selva help system. Clark Labs Clark University, USA. [www.eng.usm.my/file/27/.../IDRISI+Manual.pdf](http://www.eng.usm.my/file/27/.../IDRISI+Manual.pdf) (accessed on 12 October 2016)
- Fan W, Wei, XS, Cao YB, et al. (2017) Landslide susceptibility assessment using the certainty factor and analytic hierarchy process. *Journal of Mountain Science* 14 (5): 906-925. <https://doi.org/10.1007/s11629-016-4068-2>
- Fell R, Corominas J, Bonnard C, et al. (2008) Guidelines for landslide susceptibility, hazard and risk zoning for land-use planning. *Engineering Geology* 102(3): 99-111. <https://doi.org/10.1016/j.enggeo.2008.03.014>
- Holmgren P (1994) Multiple flow direction algorithms for runoff modelling in grid based elevation models: an empirical evaluation. *Hydrological Process* 8(4): 327-334. <https://doi.org/10.1002/hyp.3360080405>
- Horton P, Jaboyedoff M, Rudaz B, et al. (2013) Flow-R, a model for susceptibility mapping of debris flows and other gravitational hazards at a regional scale. *Natural Hazards Earth System Science* 13(4): 869-885. <https://doi.org/10.5194/nhess-13-869-2013>
- Hung O (1995) A model for the runout analysis of rapid flow slides, debris flows, and avalanches. *Canadian Geotechnical Journal* 32(4): 610-623. <https://doi.org/10.1139/t95-063>
- Imam B (2015) Bangladesh Geology. *Banglapedia - the National Encyclopedia of Bangladesh*. [http://en.banglapedia.org/index.php?title=Bangladesh\\_Geology](http://en.banglapedia.org/index.php?title=Bangladesh_Geology) (accessed on 17 November 2016)
- Iovine G, D'Ambrosio D, Di Gregorio S (2005) Applying genetic algorithms for calibrating a hexagonal cellular automata model for the simulation of debris flows characterised by strong inertial effects. *Geomorphology* 66(1): 287-303. <https://doi.org/10.1016/j.geomorph.2004.09.017>
- Kappes MS, Malet JP, Rémaitre A, et al. (2011) Assessment of debris-flow susceptibility at medium-scale in the Barcelonnette Basin, France. *Natural Hazards Earth System Science* 11(2): 627-641. <https://doi.org/10.5194/nhess-11-627-2011>
- Kayastha P, Dhital MR, De Smedt F (2013) Application of the analytical hierarchy process (AHP) for landslide susceptibility mapping: a case study from the Tinau watershed, west Nepal. *Computers & Geosciences* 52: 398-408. <https://doi.org/10.1016/j.cageo.2012.11.003>
- Kayastha P, Dhital MR, De Smedt F (2013) Evaluation of the consistency of landslide susceptibility mapping: a case study from the Kankai watershed in east Nepal. *Landslides* 10(6): 785-799. <https://doi.org/10.1007/s10346-012-0361-5>
- Kayastha P, Dhital MR, De Smedt F (2012) Landslide susceptibility mapping using the weight of evidence method in the Tinau watershed, Nepal. *Natural Hazards* 63(2): 479-498. <https://doi.org/10.1007/s11069-012-0163-z>
- Malczewski J (2004) GIS-based land-use suitability analysis: a critical overview. *Progress in Planning* 62(1): 3-65. <https://doi.org/10.1016/j.progress.2003.09.002>
- Meten M, Bhandary NP, Yatabe R. (2015) GIS-based frequency ratio and logistic regression modelling for landslide susceptibility mapping of Debre Sina area in central Ethiopia. *Journal of Mountain Science* 12 (6): 1355-1372. <https://doi.org/10.1007/s11629-015-3464-3>
- Mia MT, Sultana N, Paul A (2016) Studies on the Causes, Impacts and Mitigation Strategies of Landslide in Chittagong city, Bangladesh. *Journal of Environmental Science and Natural Resource* 8(2): 1-5. <https://doi.org/10.3329/jesnr.v8i2.26854>
- Osmany SH (2014) Chittagong City. *Banglapedia - the National Encyclopedia of Bangladesh*. [http://en.banglapedia.org/index.php?title=Chittagong\\_City](http://en.banglapedia.org/index.php?title=Chittagong_City) (accessed on 15 October 2016)
- Petrasccheck A, Kienholz H (2003) Hazard assessment and mapping of mountain risks in Switzerland. In Proceedings of the 3rd International Conference on Debris-Flow Hazards

- Mitigation. Millpress, Rotterdam. <http://www.millpress.nl/shop/abooks/DHFM/pdf/oSI.pdf> (accessed on 17 November 2016)
- Pirulli M, Mangeney A (2008) Results of back-analysis of the propagation of rock avalanches as a function of the assumed rheology. *Rock Mechanics and Rock Engineering* 41(1): 59-84. <https://doi.org/10.1007/s00603-007-0143-x>
- Prochaska AB, Santi PM, Higgins JD, Cannon SH (2008) Debris-flow runout predictions based on the average channel slope (ACS). *Engineering Geology* 98(1): 29-40. <https://doi.org/10.1016/j.enggeo.2008.01.011>
- Rahman MS, Ahmed B, Huq FF, et al. (2016) Landslide inventory in an urban setting in the context of Chittagong Metropolitan Area Bangladesh. 3rd International Conference on Advances in Civil Engineering 2016 (ICACE 2016). pp 170-178.
- Rahman MS, Di L (2017) The state of the art of spaceborne remote sensing in flood management. *Natural Hazards* 85(2): 1223-1248. <https://doi.org/10.1007/s11069-016-2601-9>
- Rahman MS, Kausel T (2012) Disaster as an opportunity to enhance community resilience: lesson learnt from Chilean coast. *Journal of Bangladesh Institute of Planners* 5(1): 1-11.
- Regmi AD, Dhital M.R, Zhang JQ, et al. (2016) Landslide susceptibility assessment of the region affected by the 25 April 2015 Gorkha earthquake of Nepal. *Journal of Mountain Science* 13 (11): 1941-1957. <https://doi.org/10.1007/s11629-015-3688-2>
- Rickenmann D (2005) Runout prediction methods. In: *Debris-Flow Hazards and Related Phenomena*. Springer. pp 305-324.
- Robinson DT, Brown DG (2009) Evaluating the effects of land - use development policies on ex-urban forest cover: An integrated agent - based GIS approach. *International Journal of Geographical Information Science* 23(9): 1211-1232. <https://doi.org/10.1080/13658810802344101>
- Saaty TL (2008) Decision making with the analytic hierarchy process. *International Journal of Services Science* 1(1): 83-98. <https://doi.org/10.1504/IJSSci.2008.01759>
- Saaty TL (1977) A scaling method for priorities in hierarchical structures. *Journal of Mathematical Psychology* 15(3): 234-281. [https://doi.org/10.1016/0022-2496\(77\)90033-5](https://doi.org/10.1016/0022-2496(77)90033-5)
- Saaty TL (1980) The analytic hierarchy process: planning, priority setting, resource allocation. McGraw-Hill International Book Co. pp 6-33.
- Soeters R, van Westen CJ (1996) Landslides: Investigation and mitigation. Chapter 8-Slope instability recognition, analysis, and zonation. Transportation research board special report 247: 129-177. <https://trid.trb.org/view.aspx?id=462506> (accessed on 20 November 2016)
- Torizin J (2016) Elimination of informational redundancy in the weight of evidence method: an application to landslide susceptibility assessment. *Stochastic Environmental Research and Risk Assessment* 30(2): 635-651. <https://doi.org/10.1007/s00477-015-1077-6>
- Van Westen C, Kappes MS, Luna BQ, et al. (2014) Medium-scale multi-hazard risk assessment of gravitational processes. In: Van Asch T, Corominas J, Greiving S, et al. (eds) *Mountain risks: from prediction to management and governance. Advances in Natural and Technological Hazards Research*, Springer, Dordrecht. pp 201-231. [https://doi.org/10.1007/978-94-007-6769-0\\_7](https://doi.org/10.1007/978-94-007-6769-0_7)
- Van Westen CJ, Castellanos E, Kuriakose SL (2008) Spatial data for landslide susceptibility, hazard, and vulnerability assessment: an overview. *Engineering Geology* 102(3): 112-131. <https://doi.org/10.1016/j.enggeo.2008.03.010>
- Van Westen CJ, Van Asch TW, Soeters R (2006) Landslide hazard and risk zonation - why is it still so difficult? *Bulleting of Engineering Geological and Environment* 65(2): 167-184. <https://doi.org/10.1007/s10064-005-0023-0>
- Vijith H, Krishnakumar KN, Pradeep GS, et al. (2014) Shallow landslide initiation susceptibility mapping by GIS-based weights-of-evidence analysis of multi-class spatial data-sets: a case study from the natural sloping terrain of Western Ghats, India. *Georisk Assessment and Management of Risk for Engineering System Geohazards* 8(1): 48-62. <https://doi.org/10.1080/17499518.2013.843437>
- Wilby RL, Dawson CW, Barrow EM (2002) SDSM—a decision support tool for the assessment of regional climate change impacts. *Environmental Modeling Software* 17(2): 145-157. [https://doi.org/10.1016/S1364-8152\(01\)00060-3](https://doi.org/10.1016/S1364-8152(01)00060-3)
- Willenberg H, Eberhardt E, Loew S, et al. (2009) Hazard assessment and runout analysis for an unstable rock slope above an industrial site in the Riviera valley, Switzerland. *Landslides* 6(2): 111-119. <https://doi.org/10.1007/s10346-009-0146-7>
- Wong HN, Ho KKS (1996) Travel distance of landslide debris. In: Senneset K, Balkema AA, Rotterdam (eds.), *Proceedings of the 7th International Symposium on Landslides*, 17-21 June 1996, Trondheim, Norway. pp 417-422.
- Zahra T (2010) Quantifying uncertainties in Landslide Runout Modelling. International Institute for Geo-information Science and Earth Observation, Netherlands. [https://www.itc.nl/library/papers\\_2010/msc/aes/zahra.pdf](https://www.itc.nl/library/papers_2010/msc/aes/zahra.pdf) (accessed on 20 December 2016)
- Zimmermann HJ (1991) Fuzzy set theory—and its applications. Springer Science & Business Media. <https://doi.org/10.1007/978-94-015-7949-0>